TECHNICAL ARTICLE

A New Class of Robust Sub-nanosecond TOF Detectors with High Dynamic Range

Dick Stresau, Kevin Hunter, Wayne Sheils, Peter Raffin and Yair Benari

ETP, Sydney, Australia
Presented at the 54th ASMS Conference on Mass Spectroscopy, Seattle, Washington, 2006

Four years ago ETP had the vision to develop a superior TOF detector. The project objectives were very simple:

- Less than 1 nanosecond pulse width
- To retain all of the advances in TOF detector technology ETP has made during the past several years (reported in various presentations to this meeting)

The result of this work is the new MagneTOF™ detector. Figure 1 shows the pulse shape from the new detector showing the typical pulse width of ~400 ps.

It clearly exceeds our initial objectives. Notice that the ring is minimized to ~1%.

ETP TOF detectors have become the preferred detector for many applications during the past 14 years because of their advantages over the alternative MCP detectors. These distinguishing advantages were included in the design objectives for the MagneTOF™ and are summarized:

- High linear pulse output current
- High linear sustained output current
- Fast recovery after ion burst
- Full performance immediately after pump-down • High pressure operation
- Low noise
- Long life
- Robust construction

The most useful and important features are the detector's linearity at high signal levels and its ease of use.

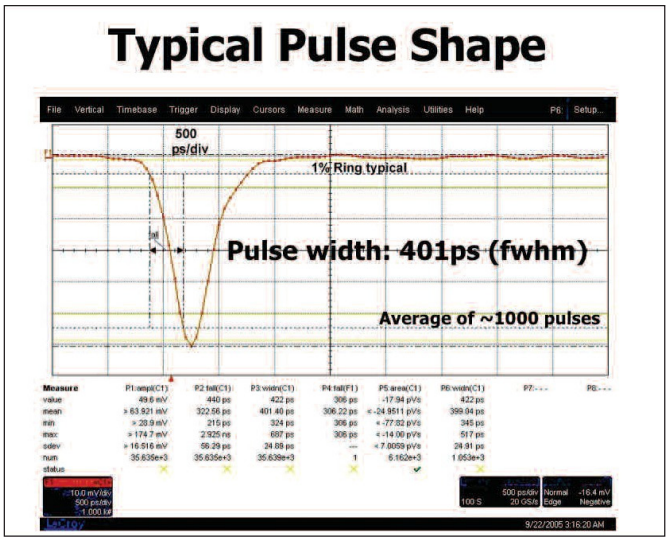

Figure 1. The typical pulse shape obtained using the DM167 Prototype Prototype MagneTOF™ electron multiplier.

Until now wide pulse width has been the only limitation for ETP TOF detectors, limiting their use in a number of applications. To overcome this limitation a number of new technologies were developed.

The key technology for achieving very narrow pulse widths has been the use of magnetic deflection for inter-dynode electron transfer.

The diagram in Figure 2 could have been taken from a first year physics text book. It shows the near toroidal trajectories of charged particles in crossed magnetic and electrostatic fields. In this diagram the particles have initial velocities expected from secondary electrons (generated from ion or electron impact).

There are a number of very useful characteristics of this process that are not immediately apparent.

The most "magical" of these is the almost total lack of time distortion in electron transit times from the emission surface to the target surface. In near uniform magnetic and electrostatic fields (as used in the amplifying section of the new detector) inter-dynode electron time dispersion is on the order of 10 picoseconds.

We are not the first group to use these concepts in a particle detector. In the early '60's the very prolific Bendix group developed these concepts into a commercial detector. (Figure 3)1

This was the same group that developed the first commercial TOF system, the channeltron detector and the MCP.

The significant drawback of this early design was that each individual dynode surface must be the same size as the input aperture. A useful detector of

this design using today's input aperture requirements would be so large as to be impractical. This limitation has been overcome by utilizing non-uniform magnetic fields.

Two important things have changed since the 1960's tomake this basic approach practical once again:

- The need for a very fast particle detector
- Easily accessible, very powerful computers: PCs

Figure 4 shows ETP's solution to the need for computing power. It's a cluster of 8 PC's which gives us the equivalent computing power of a "20 GHz Pentium". It enables the analysis and development of very complex magnetic and electrostatic structures fast enough to enable interactive modeling.

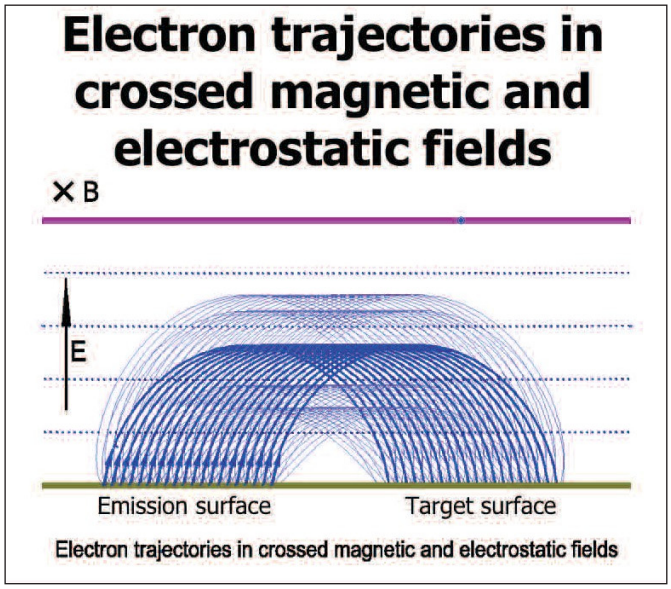

Figure 2: Electron trajectories in crossed magnetic and electrostatic fields.

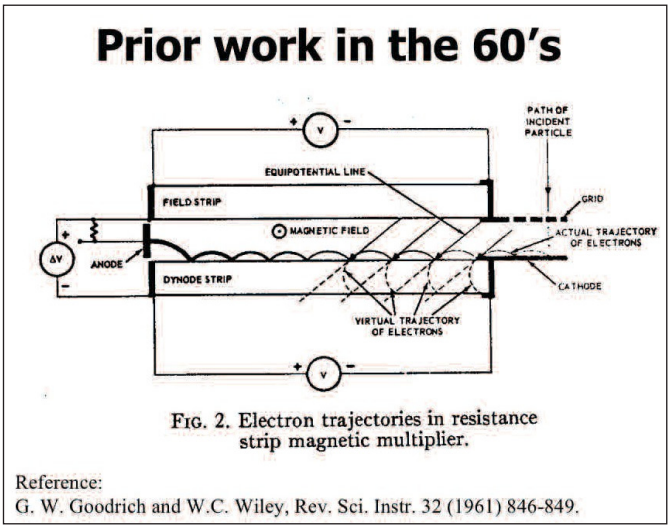

Figure 3: Earlier work in the field by Goodrich and Wiley.1

Figure 4: ETP's cluster computer - a solution to the need for powerful computing for modeling

Figure 5 shows the basic optics arrangement of the new detector. The thick black lines show the basic mechanical structure and green lines electrostatic equipotentials. The red lines indicate input ion trajectories and the blue lines secondary electron trajectories.

It's worth pointing out a number of features:

1. An outer grid, which can be fixed at a user-defined voltage (within ±5 kV of the applied -HV), is included in the design for ease of integration into a TOF system.
2. The ion input grids are made from parallel wires stretched over a flat frame enabling precision control over transmission to 92%.
3. To take advantage of narrow pulse width it is important to minimize jitter and arrange for minimum disturbance to the input ions as they pass through the detector to the impact surface. To achieve this:
    a. A significant effort has been given to design for a very uniform electrostatic field in the ion transit area. The small "kick-up" at the right end of the ion impact plate is an example of the design details included to achieve this goal.
    b. Each internal transmission grid is equipped with a compensation aperture which compensates for edge effects from field penetration through the grid.
    c. The ion impact surface is made from 3 mm thick stainless steel (coated with appropriate dynode materials). This allows for an unusually flat ion impact surface: ±10 micrometers is standard, ±5 or smaller is optional.
    d. The grids are made from parallel wires stretched over a flat frame enabling very flat grid surfaces.

Figure 6 is a view of the optics, showing contour lines of equal magnetic field strength in blue and red. This clearly shows the complex non-uniform nature of the magnetic field. This non- uniform field focuses the electrons from the large ion impact surface to the smaller second dynode, as seen from the electron trajectories in green.

Figure 7 shows an example of the simulations arranged to analyze the time distortion or jitter resulting from aperture edge effects and field penetration through the entry grids. It was necessary to carry out the simulation with a 6 micrometer array spacing to achieve accurate results.

Because these are ion arrival times the results are dependant on the ion's mass and energy. The analysis was done with 5 keV, 10,000 amu ions as a worst case scenario. Small, energetic ions will have negligible jitter.

This type of analysis was used to determine the optimal voltages to be applied to the compensation apertures to achieve minimal distortion.

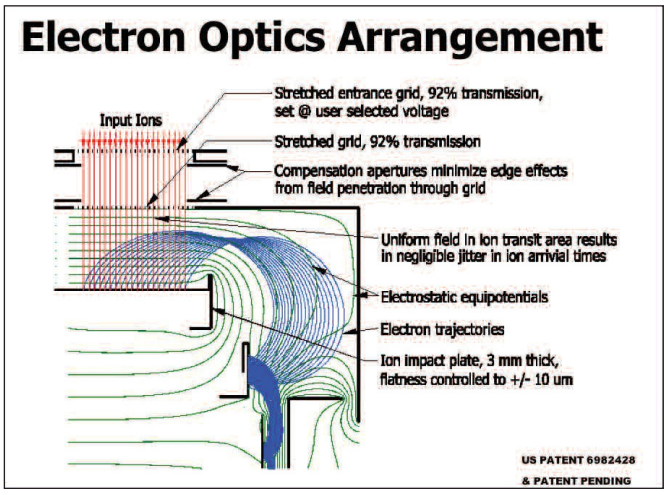

Figure 5: The electron optics arrangement for DM167 Prototype MagneTOF™.

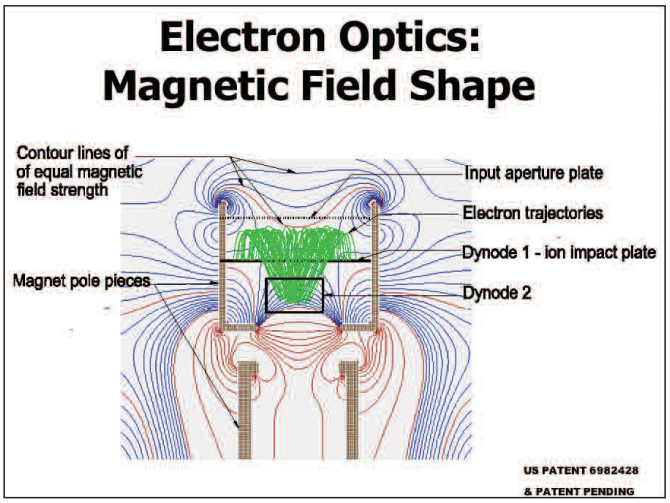

Figure 6: A view of the optics of DM167 Prototype MagneTOF™, showing the magnetic field shape

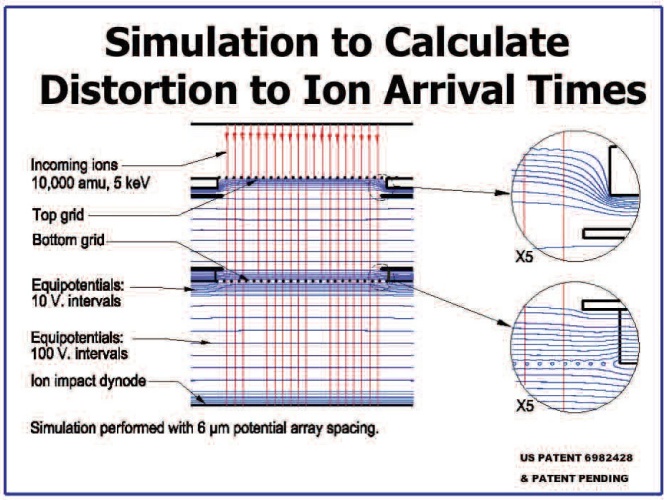

Figure 7: An example of the simulations arranged to analyze the time distortion resulting from aperture edge effects and field penetration

Figure 8 shows results from the distortion analysis showing ion arrival time as a function of position on the ion impact surface. There is less than 50 picosecond jitter across the surface except at the very edges of the aperture where it reaches ~100 picoseconds. Note that "DM167 Prototype" is the version number given to the MagneTOF™ detector used to collect this data.

The outer grid of the detector can be set to an arbitrary voltage selected by the user (within ± 5 kV of the applied -HV). This analysis was done with the outer grid attached to the detector's -HV.

Figure 9 shows the same analysis, but now the outer grid is set at the detector's +HV potential or earth for non-floating applications.

Note again that the analysis was carried out with worst case conditions of 10,000 amu ions with 5 keV energy.

The most realistic exercise devised for this detector in our lab is the "ion burst test". It is a realistic measure of the performance one can expect from this detector during a very high abundance TOF spectrum (Figure 10).

For this investigation the detector was exposed to 5 microsecond bursts of ions with a 1% duty cycle. The incident ion rate was increased until a variation of multiplier gain was observed during the ion burst. The lower trace is the average of ~2500 ion bursts and hence indicates the average detector output current, and therefore instantaneous detector gain, during the burst.

The calculations on Figure 10 show how this data corresponds to linear response during an ion burst of 300,000 ions.

The detector's averaged output of 30 mV (or 600 µA into 50 Ohms) during the 5 microsecond burst is the equivalent of an ion input rate of 6 X 1010 ions per second (for 1 mV single-ion- pulses). This corresponds to a total of 300,000 ions during the burst. From the data it is apparent that this ion burst rate has negligible influence on detector gain for the first microsecond followed by a minor gain increase (corresponding to the detector's over response at very high currents).

Work is continuing in this area and it is anticipated further improvement in the ion burst performance of the MagneTOF™ detector will be achieved.

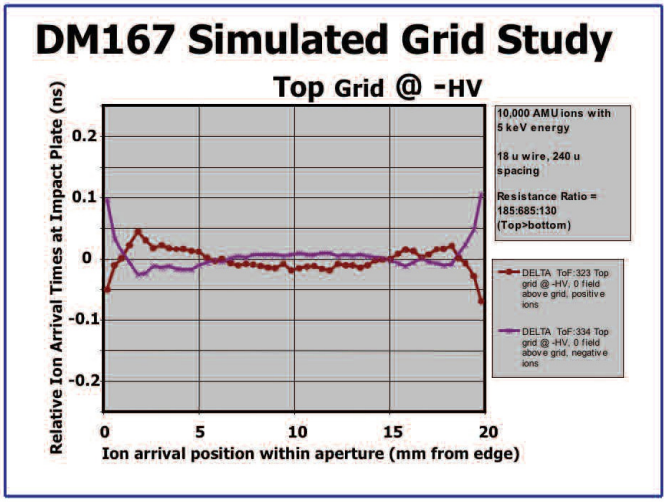

Figure 8: The results from the distortion analysis showing ion arrival time as a function of position on the ion impact surface (outer grid attached to the detector's -HV)

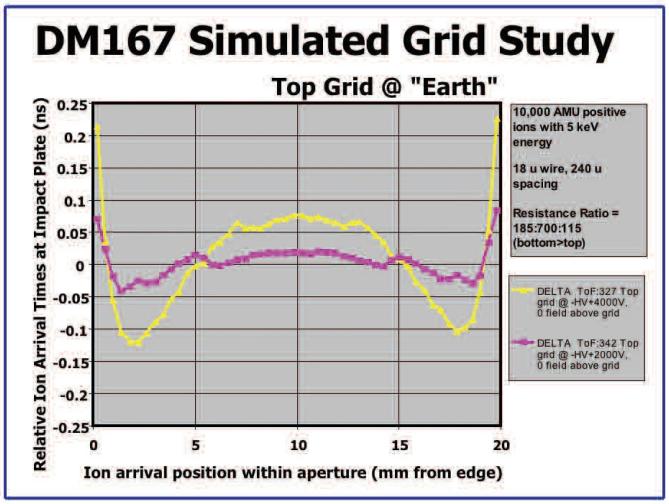

Figure 9: The results from the distortion analysis showing ion arrival time as a function of position on the ion impact surface (outer grid attached to the detector's +HV, or earth for non-floating operation).

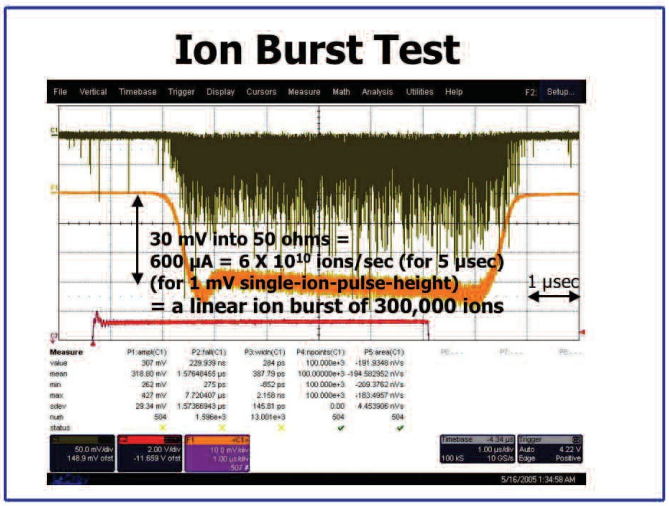

Figure 10: The ETP ion burst test is a realistic measure of the performance that can be expected from the DM167 Prototype MagneTOF™ detector during a very high abundance TOF spectrum acquisition.

Figure 11 shows a real example of serendipity. The objective was to achieve an operational life equivalent to that of "standard" ETP electron multipliers. The observed aging rate is considerably lower than any previous ETP electron multiplier or that reported for any electron multiplier.

To approximate the expected operating life of the MagneTOF™ it was operated in a system that periodically adjusted the applied high voltage to maintain a gain of 2 X 105 (~3 mV single ion pulse height into 50 ohms).

The blue curve shows the voltage required to maintain this gain and indicates negligible aging for >1 coulomb of accumulated output charge.

The input ion beam was operated with a 50% duty cycle (50 ms on, 50 ms off) to approximate somewhat normal usage conditions. During the beam-on state the detector output current was maintained at ~10µA (corresponding to ~3X108 ions/second of input ion flux, within the detector's linear operating range). This experiment was conducted in a chamber pumped with a turbo pump-diaphragm pump system to a pressure of 5 X 10-6 torr.

Work is continuing on understanding the mechanisms involved in this result and it is expected to be utilized in other application areas.

Figure 12 shows the typical pulse height distribution of the new detector. It has an unusual shape as a result of the very high secondary electron yield from the second dynode. This enables the resolution of individual peaks resulting from the Poisson distribution of the number of secondary electrons generated by ion impact on the first dynode.

The dark blue blocks show the Poisson distribution for a mean of 2.0 events. This is the expected distribution of the number of electrons emitted from an ion impact with an average yield of 2, which is appropriate for the 30 amu, 3 keV ions used to collect this data.

The distribution is dominated by the ion impact secondary yield characteristics and therefore is as narrow as can be expected from a non-saturating detector. A larger yield and thus narrower distribution can be expected from higher energy ions.

Figure 13 shows a plateau curve generated with the new detector using the conventional method of increasing the applied HV in steps and recording the output count rate while exposing the detector to a fixed flux of input ions.

This is the standard method used for setting the appropriate HV for most pulse counting and TOF systems.

When the HV is set to just above the "knee" (~2.9 kV in the 1 mV case) it can be assumed that essentially all of the ions have been detected that have generated pulses within the detector.

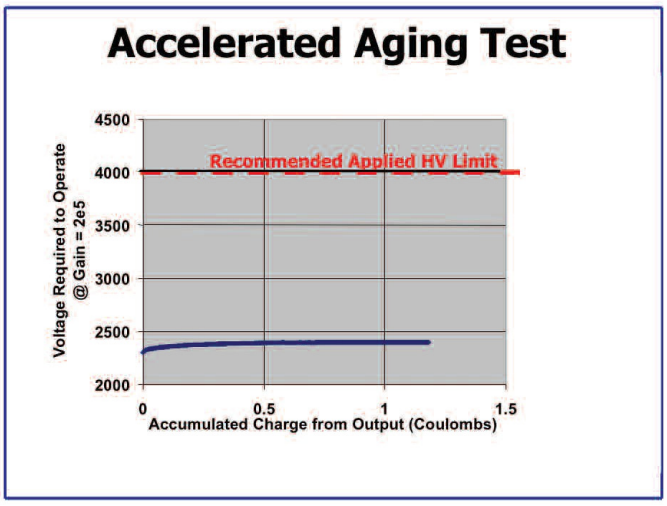

Figure 11: An aging test shows that the DM167 Prototype MagneTOF™ multiplier lifetime is far greater than reported for any other electron multiplier.

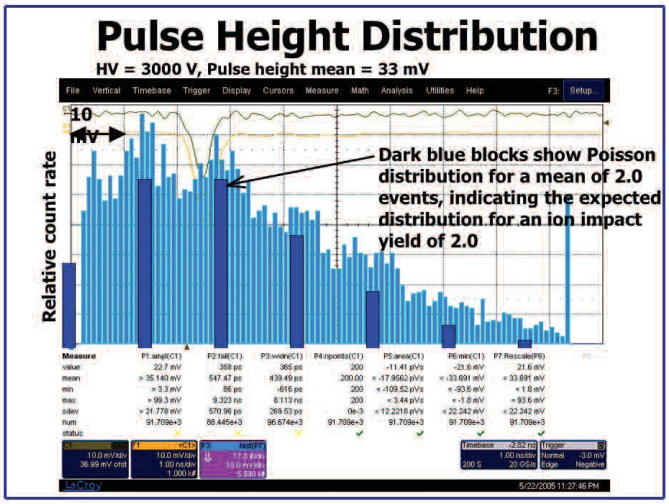

Figure 12: Typical pulse height distribution of the MagneTOF™ detector.

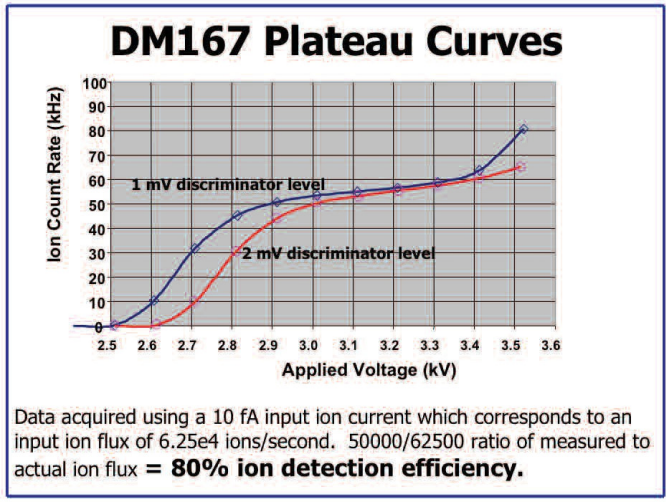

Figure 13: Plateau curves generated using the new MagneTOF™ detector.

The input ion current can also be measured. Converting this to an input ion rate enables calculation of the detector's absolute ion detection efficiency as the ratio of the two measurements.

Applying this procedure to this data results in an 80% ion detection efficiency, which is very close to the value expected from grid transmission and Poisson statistics.

The detector on the right of the photograph in Figure 14 is the DM167 Prototype version of the MagneTOF™, that has been used to collect the data in this paper. To give an idea of scale: its ion entrance aperture, at the top, is 15 X 33 mm.

Following the success with the DM167 Prototype a more compact, lower cost version of the detector was designed. The resulting DM291, on the left in Figure 14, has a 10 X 25 mm aperture and has ~1 ns pulse width.

In the foreground is the DM345 AC Signal Coupling unit, which can be attached to either version and provides 15 kV isolation of the output signal from the rest of the unit.

Summary of the DM167 Prototype MagneTOF™ detector's characteristics:

- 400 picosecond pulse width (FWHM)
- Linear response:
  - During and after a burst of 300,000 ions
  - 1 Volt output pulse (into 50 ohms)
  - 10 microamp sustained output current
  - For spatially concentrated ion beams
- Exceptional operating life
- Very flat ion impact surface: ±10 micron (± 5 micron or less optional)
- Full performance just after pump-down
- No special storage requirements

So what is the future for this technology? How fast can it go?

To get a feel for how well the technology follows the basic design assumptions, a few of the operational parameters were pushed to their extreme.

Figure 14: The new MagneTOF™ range of electron multipliers and accessories.

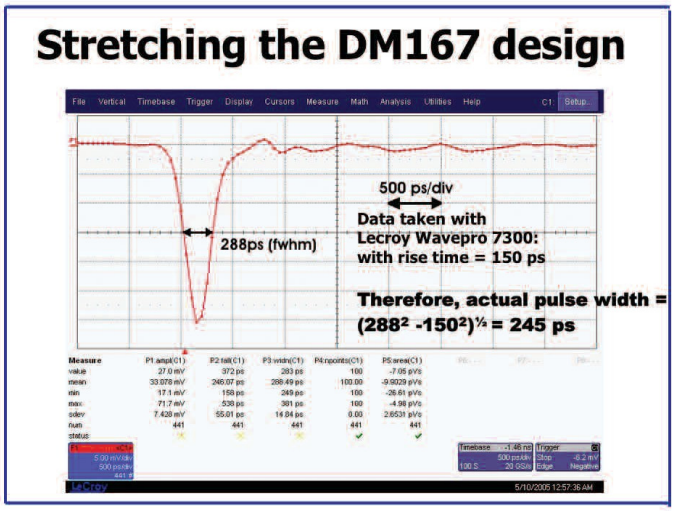

Figure 15: By pushing various design parameters to their extreme the MagneTOF™ detector achieved a pulse width of 250 picoseconds!

This resulted in a 250 picosecond pulse width. (Figure 15).

To date no fundamental limits for speed have been reached with the MagneTOF™ detector.

100ps looks achievable if chosen as a design objective.

This may become important for future TOF systems.

CONCLUSIONS

- The MagneTOF™ detector exhibits 400 ps pulse width as well as all the dynamic range and robust features of ETP detectors (outlined above).
- The new MagneTOF™ detector eliminates the compromises associated with previous TOF detectors.
- The new technology will continue to meet the demand for ever-increasing TOF detector performance.

ACKNOWLEDGEMENTS

Thanks to Hermann Wollnik who offered valuable ideas and insight into many important details at various stages of this project.

REFERENCES

1. G. W. Goodrich and W.C. Wiley, Rev. Sci. Instr. 32 (1961) 846-849

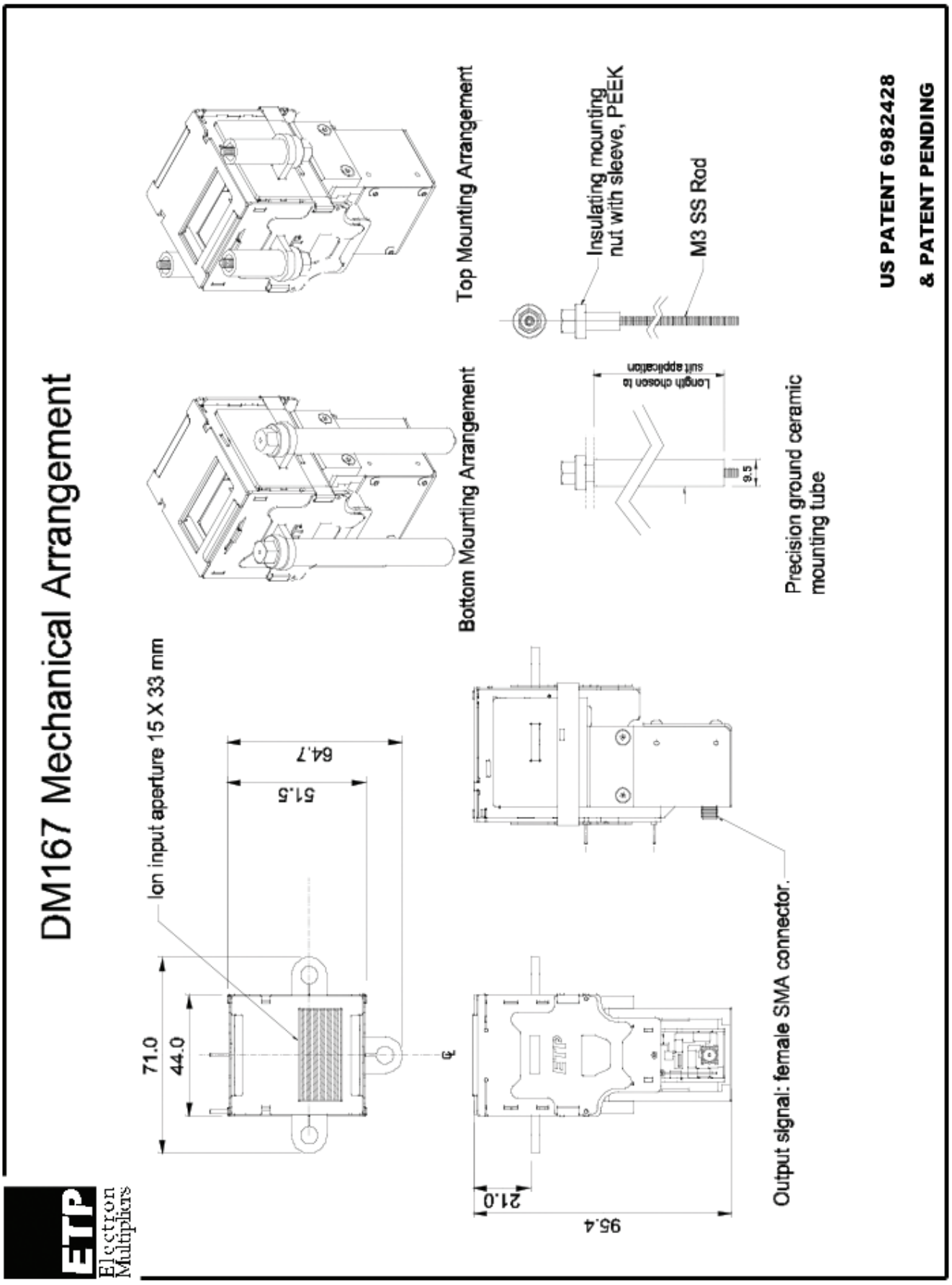

Figure 16: The mechanical arrangement of the DM167 Prototype MagneTOF™ electron multiplier.

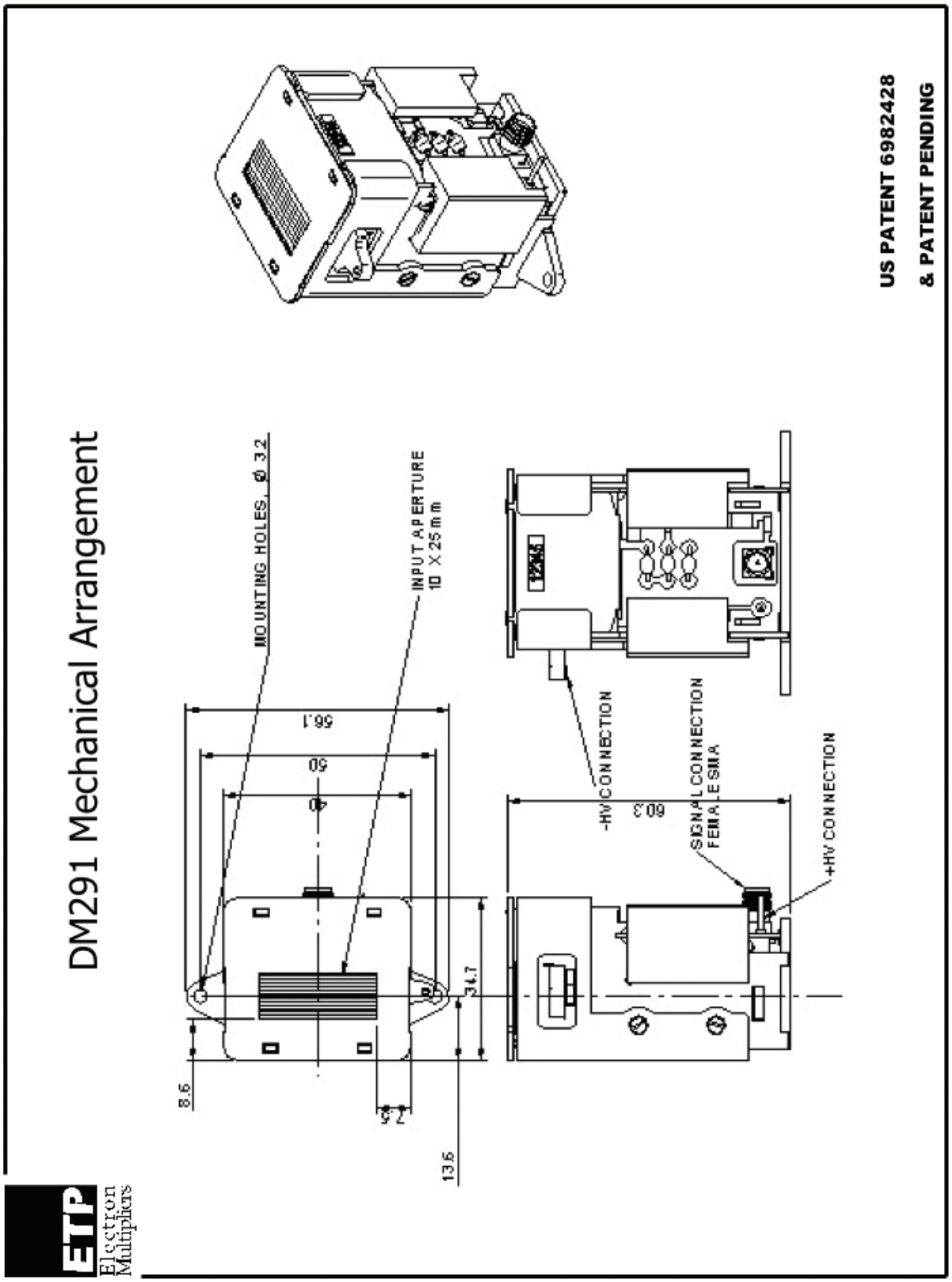

Figure 17: The mechanical arrangement of the DM 291 Prototype MagneTOF™ electron multiplier.

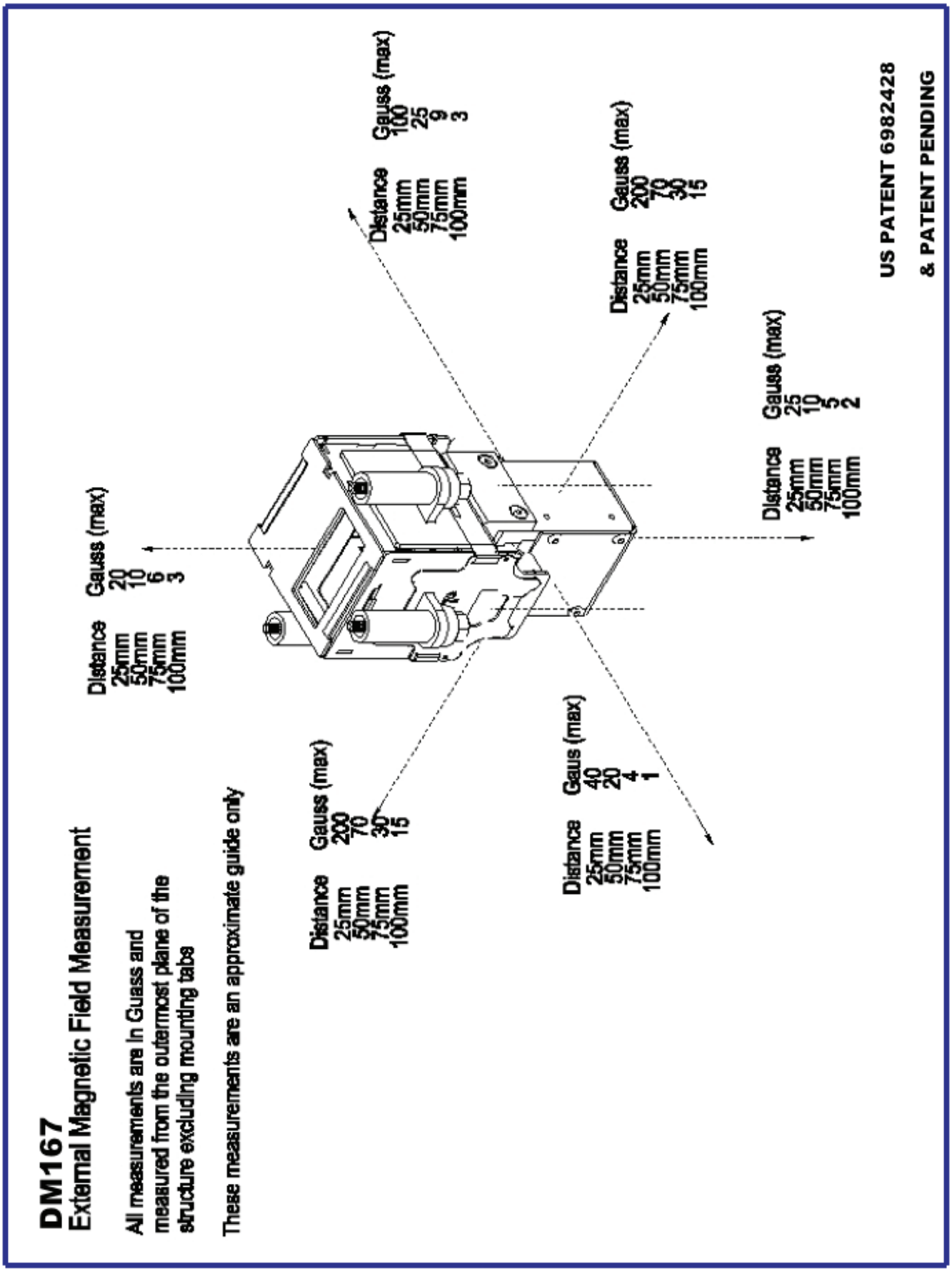

Figure 18: The external magnetic field measurement of the DM167 Prototype MagneTOF™ electron multiplier.

TABLE 1

SPECIFICATIONS	DM167 PROTOTYPE	DM291 PROTOTYPE
Multiple ion pulse width (FWHM) (ns)	<0.5	<1.0
Input aperture size (mm)	15 X 33	10 X 25
Mechanical envelope size (mm)[1]	44 X 52 X 96	38 X 40 X 60
Linear response:	During & after a burst of 300,000 ions	
Linear response:	>1 Volt output pulse (into 50 Ohms)	
Linear response:	10 µA sustained output current	
Linear response:	For spatially concentrated ion beams	
Impact surface flatness:	±10 µm (±5 µm or less optional)	
Maximum dark counts:	20 per minute @ 3000 Volts	
Recovery time after large pulse:	Negligible	
Maximum operating pressure:	10-4 Torr	
Long/short term storage requirements:	Protect from dust	
Ion detection efficiency (low mass):	80%	
Conditioning time after pumpdown:	None	
Operating voltage[2]:	~2500 (initial) to 4000 (aged)	
Typical gain at 2500 volts:	105 = ~1 mV into 50 Ohms	

1. Mounting tabs protrude beyond each of these envelope sizes.
2. Up to 0.5 mA will be drawn from the HV power supply.

Table 1: The preliminary specifications for the MagneTOF™ range of electron multipliers.

ETP electron multipliers

ETP Electron Multipliers
ABN: 35 078 955 521
Address: 31 Hope Street,
Melrose Park NSW 2114
Australia
Tel: +61 (0)2 8876 0100
Fax: +61 (0)2 8876 0199
Email: info@etp-ms.com
Web: www.etp-ms.com